Segmentation of Lung Field in HRCT Images using U-Net Based Fully Convolutional Networks

Abhishek Kumar[1], Sunita Agarwala[2], Ashis Kumar Dhara[3], Debashis Nandi[2], Sumitra Basu Thakur[4], Ashok Kumar Bhadra[4] and Anup Sadhu[4]

[1]School of Computer and Information Sciences University of Hyderabad, INDIA.
[2]Computer Science & Engineering, National Institute of Technology Durgapur,INDIA.
[3]Centre for Image Analysis, Uppsala University, SE-751 05 Uppsala, SWEDEN.
[4]Medical College Kolkata,INDIA.

Abstract. Segmentation is a preliminary step towards the development of automated computer aided diagnosis system (CAD). The system accuracy and efficiency primarily depend on the accurate segmentation result. Effective lung field segmentation is major challenging task, especially in the presence of different types of interstitial lung diseases (ILD). At present, high resolution computed tomography (HRCT) is considered to be the best imaging modality to observe ILD patterns. The most common patterns based on their textural appearances are consolidation, emphysema, fibrosis, ground glass opacity (GGO), reticulation and micronodules. In this paper, automatic lung field segmentation of pathological lung has been done using U-Net based deep convolutional networks. Our proposed model has been evaluated on publicly available MedGIFT database. The segmentation result was evaluated in terms of the dice similarity coefficient (DSC). Finally, the experimental results obtained on 330 testing images of different patterns achieving 94% of average DSC.

1 INTRODUCTION

Many different pulmonary disorders, generally exhibiting similar clinical manifestations are combined together into one group called as interstitial lung disease (ILD). They mainly affect the tissue and space near the alveoli also called interstitium making it inflamed and stiff, which further affects the exchange of air into the bloodstream. If these diseases diagnosed early there is a chance of speedy recovery, otherwise if remains untreated for a longer period of time they may turn into life threatening complications. The survival rate varies for different disorders and the most common disorder among them is Idiopathic pulmonary fibrosis. The rate of survival is 2 to 3 years for Idiopathic pulmonary fibrosis [1]. ILD tissues are classified into various patterns. The six patterns are most common and significant namely, consolidation, emphysema, fibrosis, ground glass opacity (GGO), micro-nodule, reticulation as shown in Figure 1.

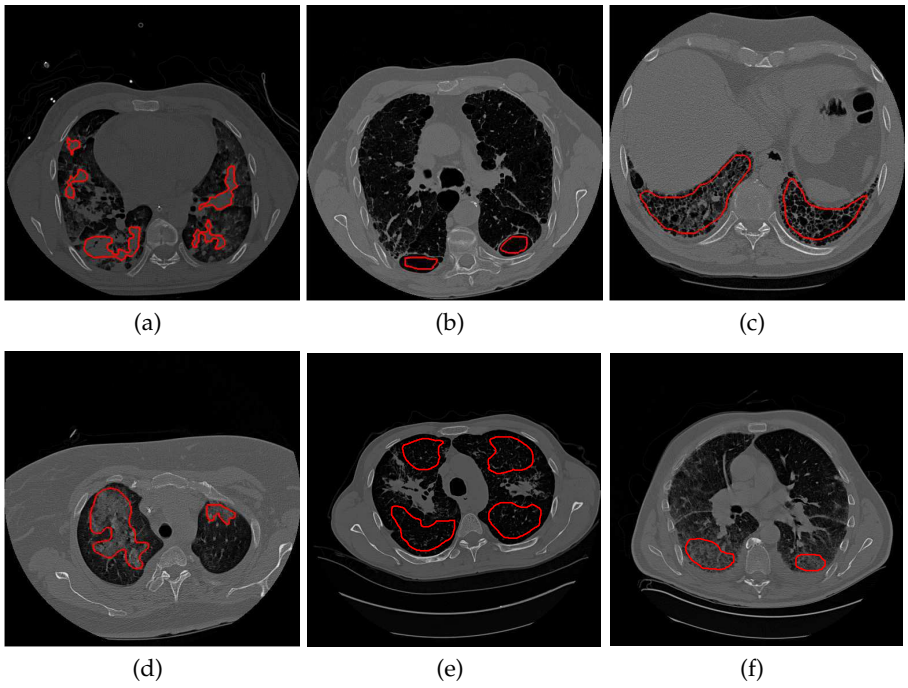

Fig. 1: Different type of ILD patterns: (a) consolidation (b) emphysema (c) fibrosis (d) ground glass opacity (e) micronodule and (f) reticulation

The world prevalence of ILD disease is 595,000 [1] and resulted deaths approximately 471,000 [2] peoples in 2013. Although ILDs constitutes more than 200 different diseases they tend to exhibits same clinical manifestations and there is ambiguity in patterns also. High resolution computed tomography (HRCT) imaging modality is preferred over computed tomography (CT) for diagnosis of ILD patterns because of its high resolution which makes the pattern observation easier for radiologists. Normally, there may be 100 to 150 HRCT slices for a single patient. So analyzing such a huge amount of data and making an accurate diagnosis is a difficult task. Moreover, two things make this task even more difficult: first, most of the patterns look similar so identifying between different patterns is difficult even for expert radiologists and second in cases where more than one pattern is present in the same lung field. So, there is a need to develop an automatic computer aided diagnosis (CAD) system for localizing and segmenting the lung field in order to have a better understanding of ILD patterns. The accurate and efficient lung field segmentation is the first task of any CAD system which is being developed for identification of ILD patterns. Majority of the lung segmentation methods does not give desired results when coming across pathological lung field. The presence of homogeneous anatomical structures around lung region further

affect the accuracy of segmentation algorithms. A CAD system for ILD classification basically consists of four steps: (a) lung field localization (b) lung field segmentation (c) detection of ILD patterns (d) classification of detected patterns.
This paper mainly focuses on the first two parts *i.e*. lung field localization and segmentation using U-Net architecture. A lot of classical techniques of segmentation already exists such as threshold-based [3], region growing [4, 5], fuzzy techniques [6] etc. but most of them do not give the desired output if dense pathology is present in the lung field. In [7], some functionalities of CNNs had been used. Gradient descent was used to train the network in a supervised manner. However, a modified RBM was used for classification and feature extraction. In [8], automated active shape model has been used given by [9]. Multiple atlases were first created and then training of active shape model is done with the help of these atlases. Because of the use of prior shape, the method is giving good results but the data size is very small, so its accuracy on a bigger dataset need to be tested. Recently, deep learning based image localization and segmentation methods caught the eyes of researchers due to their impressive performance in several image processing competitions held worldwide. The advancement in technology such as more advanced GPU, better hardware also contributed to the designing and successful implementation of more complex network architectures such as VGG, ResNet etc. In this paper, the computational power of deep CNN has been utilized for automated segmentation of lung field using U-Net.

2 MATERIALS AND METHODOLOGY

2.1 Dataset Description

The proposed work is evaluated on publicly available MedGIFT database [10] for ILD patterns. A total of 1030 images have been taken out of which 700 images used for training purposes. The number of training images have been further increased using data augmentation techniques. The overall dataset description is given in Table 1.

2.2 Network Architecture

Our network architecture is based on U-Net architecture originally designed by Olaf Ronneberger et al. [11]. The authors were the winners at ISBI cell tracking challenge 2015 by a huge margin with the help of same architecture. It is a common belief, that to achieve the good result with deep convolutional networks a good amount of training data is required. The impressive results shown by most of the networks trained on larger datasets also confirms this fact. But most of these networks were originally designed for natural color images where the amount of good quality annotated data is not an issue. But, in case of medical image processing, the availability of good quality annotated

Table 1: HRCT data of different patterns obtained from MedGIFT database

Lung Tissue Patterns	**No of training image**	**No of testing image**	**Total no of image**
Consolidation	80	36	116
Emphysema	50	21	71
Fibrosis	183	110	293
GGO	168	73	241
Healthy	49	20	69
Micronodule	108	46	154
Reticulation	62	24	86
Total	700	330	1030

data always remains an issue. The U-Net architecture fills this gap by giving good results with a lesser number of data. The base of U-Net architecture is actually built upon a fully convolutional network given by [12]. The design consists of two parts: the first part is the contracting part and the second part is expansive part and both the parts are fully symmetrical giving the architecture a U-shape. Our proposed model which is based on U-Net consists of two parts decreasing path followed by increasing path as shown in Figure 2. The decreasing path resembles the architecture of a traditional convolutional network. It consists of two 3x3 convolutions used repeatedly followed by a rectified linear unit (ReLU) and a 2x2 max pooling operation with stride 2. A padding of 1 has been used while original U-Net architecture was unpadded. The number of feature channels doubles itself upto start of increasing path. The increasing path is almost symmetrical to the decreasing path just reverse in nature. A 2x2 convolution has been used to half the number of feature channels and two 3x3 convolutions followed by a ReLU activation function. A 1x1 convolution has been used to map the feature vector with the number of classes.

2.3 Training of U-Net

The network was trained using 2800 HRCT images and tested on 330 images. The training was performed on 10000 iterations and some of the important parameters are discussed below:

Data Augmentation Due to scarcity of quality annotated data in the field of biomedical image processing, data has been increased artificially using some data augmentation techniques such as translation, rotation, horizontal flip and vertical flip which increases the number of training samples and helps the network to train on a larger sample size. In our proposed method, this technique has been used to achieve better performance and reduce the chances of overfitting [13]. The increased data obtained after applying the above mentioned data augmentation techniques is shown in Table 2.

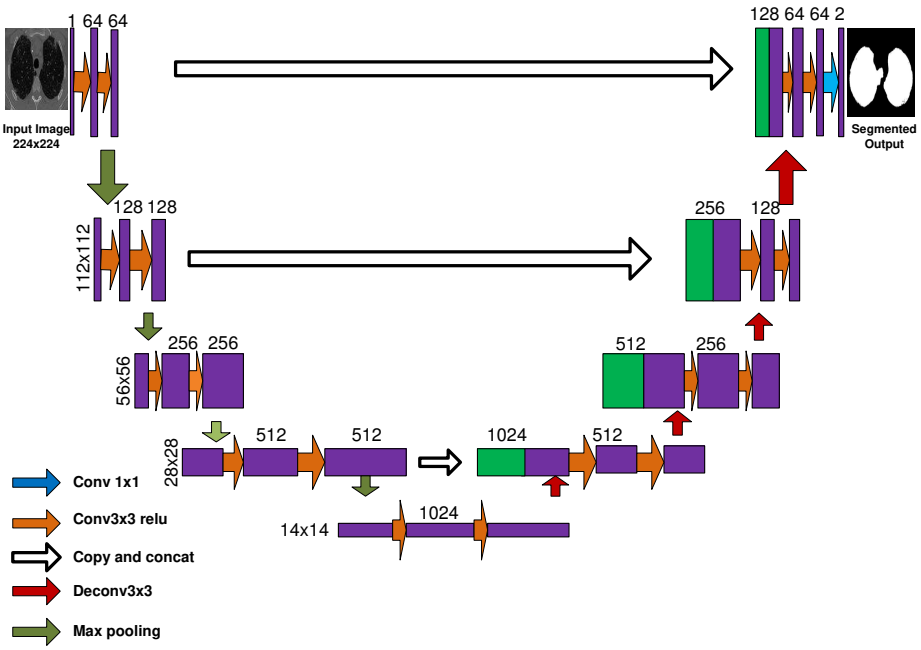

Fig. 2: Modified Fully Convoluational U-Network Architecture

Table 2: Dataset after applying image Augmentation techniques

Lung Tissue Patterns	No of training image with Augmentation	No of testing image	Total no of image
Consolidation	320	36	356
Emphysema	200	21	221
Fibrosis	732	110	842
GGO	672	73	745
Healthy	196	20	216
Micronodule	432	46	478
Reticulation	248	24	272
Total	2800	330	3130

Activation Function In neural network activation function decide whether the neuron will be fired or not. There are different types of activation function like sigmoid function, tangent function, rectified linear unit (ReLu) and leaky rectified linear unit (LReLu). ReLu has been used in this case.
Loss Function This function is significant to measure the inconsistency between the actual label and the predicted label. Cross-Entropy loss function has been used for this purpose due to its efficiency in binary classification.
Optimization Technique It is used to maximize or minimize the objective

function. There are various type of optimization techniques like gradient descent, RMSprop, Adadelta, and Adam. We have used Adam approach which is an extension of stochastic gradient descent optimization [14].

3 Experimental Setup and Results

3.1 Implementation Setup

The experimental setup is shown in Table 3. The whole setup was implemented in Linux environment using NVIDIA GTX 1070 8 GB GPU on a system with 16 GB RAM and having corei5 7th generation @3.50GHz processor. The packages like python 2.7, caffe, CUDA 8.0, cudnn, pytorch etc. are required for execution of our code based on UNet architecture.

Table 3: Experimental Environments setup

CPU	Intel (R) Core (TM) i7-4790K 4.00Hz
GPU	GeForce GTX1080 Ti
Main Memory	16 GB
Operating System	Ubuntu 16.04
Packages	pyhon 2.7, caffe, CUDA 8.0, cudnn, pytorch

3.2 Evaluation

Quantitative performance of the algorithms are reported in terms of Dice Similarity Coefficient (DSC) [15] as described below:
Let us consider two regions, whose pixels are classified as follows:

N_{tp} - Number of true positive pixels
N_{tn} - Number of true negative pixels
N_{fp} - Number of false positive pixels
N_{fn} - Number of false negative pixels

$$\mathrm{DSC} = \frac{2N_{tp}}{2N_{tp} + N_{fp} + N_{fn}} \tag{1}$$

The range of this metric lies between $0, 1$, where 0 is the worst performance and 1 being the best performance.
The proposed method is trained on 2800 normal lung HRCT images for left as well as right both lung lobes. After that, it has been tested on 330 HRCT images obtained from a publicly available database [10] having six different ILD patterns: consolidation, emphysema, fibrosis, ground glass opacity, micronodule and reticulation. The qualitative result of the proposed method with

the ground truth has been shown in Figure 3. The proposed method gives a DSC index of 0.94 when number of testing images is 330 which consists of testing images from all six patterns together. The quantitative result has been shown in Table 4 when all the patterns are given individually as testing data.

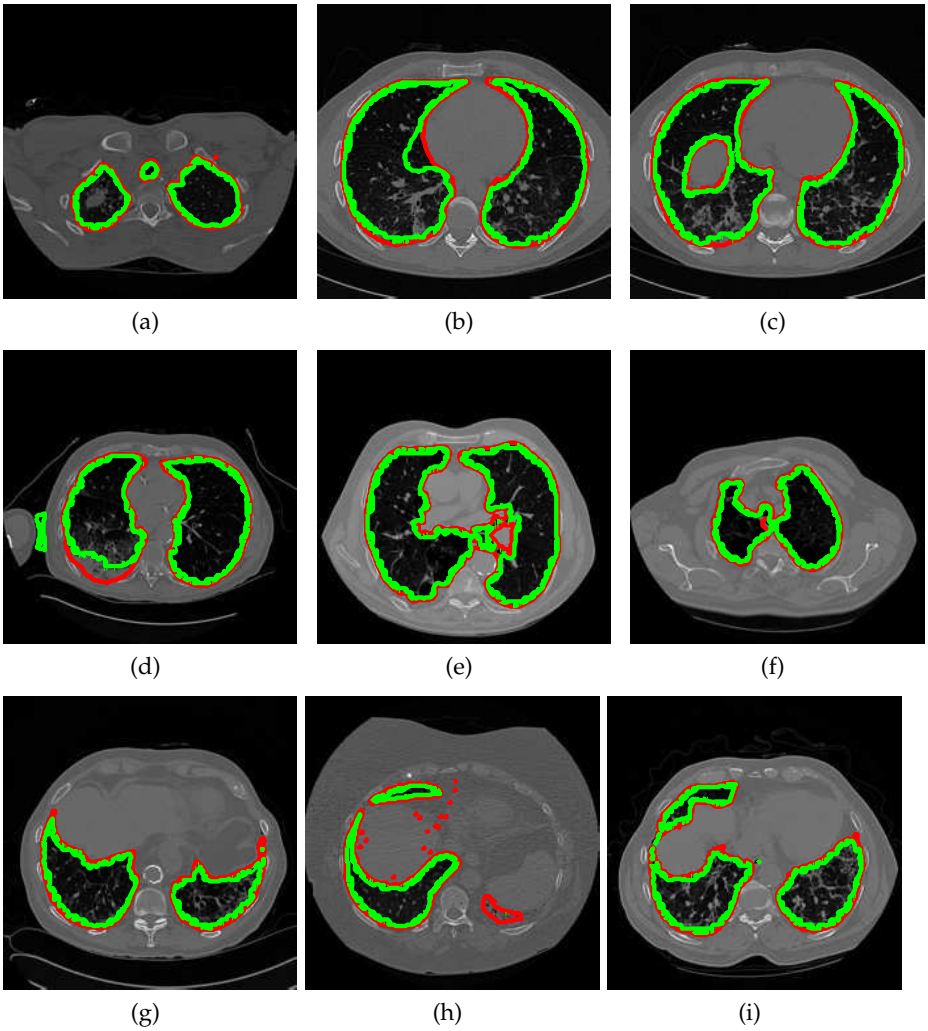

(a) (b) (c)

(d) (e) (f)

(g) (h) (i)

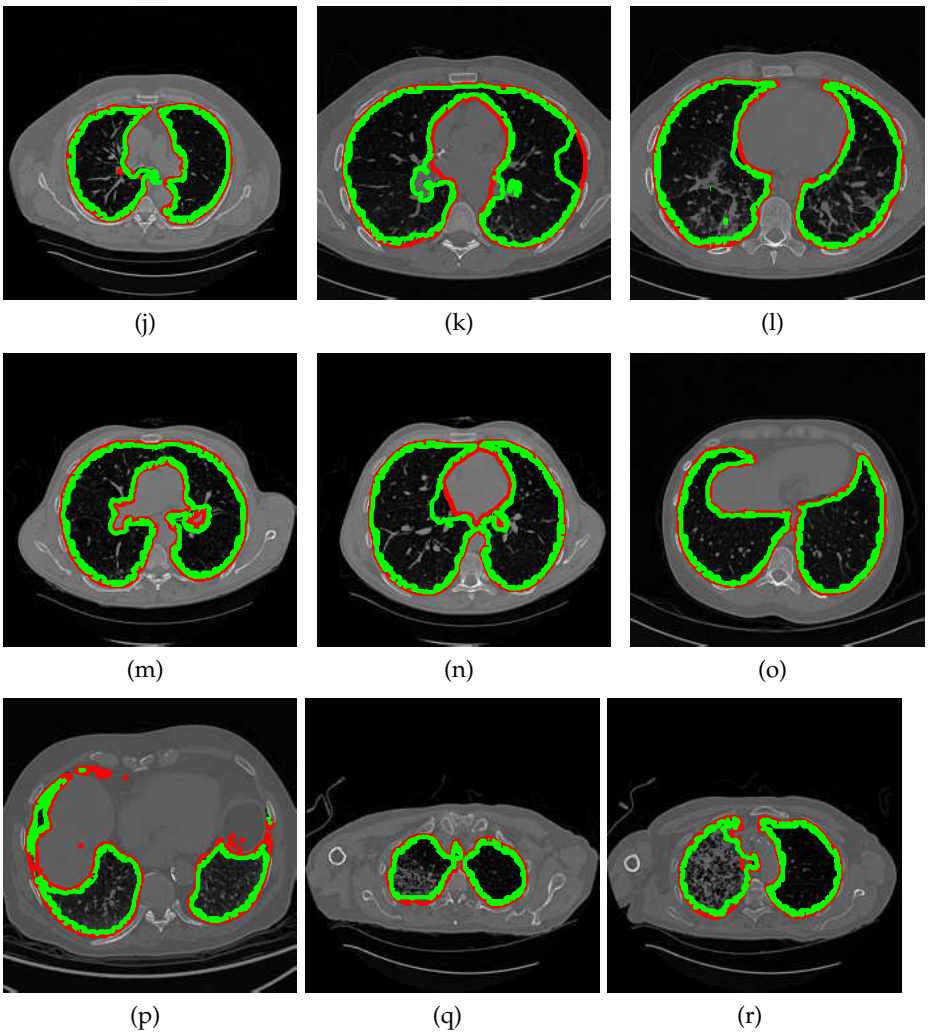

Fig. 3: Segmented output image for different patterns.(a)-(c) is the output image for consolidation, (d)-(f) is the segmented output for emphysema, (g)-(i) is the segmented output for fibrosis, (j)-(l) is the output image for GGO, (m)-(o) is the output image for micronodules and, (p)-(r) is the segmented output for reticulation. The red color line is the original ground truth boundary whereas green color line represents the segmented boundary.

3.3 Results and Discussion

In this work, an automated lung segmentation method has been proposed using deep CNN based on U-Net architecture. The network is trained using 2800

Table 4: Segmentration accuracy of different patterns in terms of DSC metric

Lung Tissue Patterns	**Training Data**	**Testing Data**	**DSC**
Consolidation	2800	36	92 %
Emphysema	2800	21	94 %
Fibrosis	2800	110	92 %
GGO	2800	73	94 %
Micronodule	2800	46	94%
Reticulation	2800	24	93 %
Average			93.1%

images obtained after applying image augmentation techniques. The network is trained for 10000 iterations for each pattern. This imageset of 2800 images is further equally divided into two parts. One part is used for training purpose and another part is used as validation set. The testing set contains 330 original images without augmentation. When all the test images are given at a time the network achieves DSC value of approximately 94% overall. Table 4 shows a quantitative result in terms of DSC metric when all the patterns are given individually. The overall average result for all the patterns together is approximately 93%. The result can be further improved by proper labeling of the database.

4 Conclusion

This paper presents an automated lung segmentation method with ILD patterns. The six major ILD patterns were taken into consideration. The power of convolutional networks has been applied with the help of U-Net architecture. The architectural design of U-Net is such that it does not require huge number of training data to train the model and because of this it is very helpful for bio-medical image processing where there is always a scarcity of quality annotated data. The segmented results has been evaluated in terms of DSC metric and it achieves an average score of approximately 93.1%. The impressive performance of the model shows that U-Net is quite capable of producing good results even with low number of data. The future work includes covering of more number of ILD patterns and further developing a CAD system which gives accurate results for complex ILD patterns.

Acknowledgments

The research is supported by National Institute of Technology, Durgapur by providing the required scientific environment and resources. The research work is funded by Visvesvaraya Ph.D. scheme of DeitY (Department of Electronics & Information Technology), Govt. of India.The authors are grateful

to Medical College Kolkata and EKO DIAGNOSTICS, Kolkata for providing valuable advice for our research work.

References

1. R. Lozano, M. Naghavi, K. Foreman, S. Lim, K. Shibuya, V. Aboyans, J. Abraham, T. Adair, R. Aggarwal, S. Y. Ahn *et al.*, "Global and regional mortality from 235 causes of death for 20 age groups in 1990 and 2010: a systematic analysis for the global burden of disease study 2010," *The Lancet*, vol. 380, no. 9859, pp. 2095–2128, 2013.
2. I. Abubakar, T. Tillmann, and A. Banerjee, "Global, regional, and national age-sex specific all-cause and cause-specific mortality for 240 causes of death, 1990-2013: a systematic analysis for the global burden of disease study 2013," *Lancet*, vol. 385, no. 9963, pp. 117–171, 2015.
3. M. S. Brown, M. F. Mcnitt-Gray, N. J. Mankovich, J. G. Goldin, J. Hiller, L. S. Wilson, and D. Aberie, "Method for segmenting chest ct image data using an anatomical model: preliminary results," *IEEE transactions on medical imaging*, vol. 16, no. 6, pp. 828–839, 1997.
4. R. Adams and L. Bischof, "Seeded region growing," *IEEE Transactions on pattern analysis and machine intelligence*, vol. 16, no. 6, pp. 641–647, 1994.
5. S. Hojjatoleslami and J. Kittler, "Region growing: a new approach," *IEEE Transactions on Image processing*, vol. 7, no. 7, pp. 1079–1084, 1998.
6. J. C. Bezdek, "Objective function clustering," in *Pattern recognition with fuzzy objective function algorithms*. Springer, 1981, pp. 43–93.
7. G. van Tulder and M. de Bruijne, "Learning features for tissue classification with the classification restricted boltzmann machine," in *International MICCAI Workshop on Medical Computer Vision*. Springer, 2014, pp. 47–58.
8. Sunita Agarwala; Debashis Nandi; Abhishek Kumar; Ashis Kumar Dhara; Sumitra Basu Thakur ; Anup Sadhu and Ashok Kumar Bhadra, "Automated segmentation of lung field in HRCT images using active shape model," in *Region 10 Conference (TENCON), 2017 IEEE*. IEEE, 2017, pp. 2516–2520.
9. T. F. Cootes, C. J. Taylor, D. H. Cooper, and J. Graham, "Active shape models-their training and application," *Computer vision and image understanding*, vol. 61, no. 1, pp. 38–59, 1995.
10. A. Depeursinge, A. Vargas, A. Platon, A. Geissbuhler, P.-A. Poletti, and H. Müller, "Building a reference multimedia database for interstitial lung diseases," *Computerized medical imaging and graphics*, vol. 36, no. 3, pp. 227–238, 2012.
11. O. Ronneberger, P. Fischer, and T. Brox, "U-net: Convolutional networks for biomedical image segmentation," in *International Conference on Medical image computing and computer-assisted intervention*. Springer, 2015, pp. 234–241.
12. J. Long, E. Shelhamer, and T. Darrell, "Fully convolutional networks for semantic segmentation," in *Proceedings of the IEEE conference on computer vision and pattern recognition*, 2015, pp. 3431–3440.
13. A. Krizhevsky, I. Sutskever, and G. E. Hinton, "Imagenet classification with deep convolutional neural networks," in *Advances in neural information processing systems*, 2012, pp. 1097–1105.
14. D. P. Kingma and J. Ba, "Adam: A method for stochastic optimization," *arXiv preprint arXiv:1412.6980*, 2014.
15. S. Mukhopadhyay, "A segmentation framework of pulmonary nodules in lung ct images," *Journal of digital imaging*, vol. 29, no. 1, pp. 86–103, 2016.